^{6}Li production by the radiative decay of long-lived particles

Motohiko Kusakabe* and Toshitaka Kajino

Department of Astronomy, School of Science, University of Tokyo, Hongo, Bunkyo-ku, Tokyo 113-0033, Japan,
and Division of Theoretical Astronomy, National Astronomical Observatory of Japan, Mitaka, Tokyo 181-8588, Japan

Grant J. Mathews

Center for Astrophysics, University of Notre Dame, Notre Dame, Indiana 46556, USA

Recent spectroscopic observations of metal-poor stars have indicated that both ^{7}Li and ^{6}Li have abundance plateaus with respect to the metallicity. Abundances of ^{7}Li are about a factor three lower than the primordial abundance predicted by standard big bang nucleosynthesis (SBBN), and ^{6}Li abundances are ~1/20 of ^{7}Li, whereas SBBN predicts negligible amounts of ^{6}Li compared to the detected level. These discrepancies suggest that ^{6}Li has another cosmological or Galactic origin than the SBBN. Furthermore, it would appear that ^{7}Li (and also ^{6}Li) has been depleted from its primordial abundance by some post-BBN processes. In this paper we study the possibility that the radiative decay of long-lived particles has affected the cosmological lithium abundances. We calculate the nonthermal nucleosynthesis associated with the radiative decay taking account both of the primary nuclear production reactions and the effects of secondary production as well as the destruction processes of energetic nuclides D, T, ^{3}He, ^{4}He, ^{6}Li, and ^{7}Li. We explore the allowed region of the parameters specifying the properties of long-lived particles. We also impose constraints from observations of the CMB energy spectrum. We find that nonthermal nucleosynthesis produces ^{6}Li at the level detected in metal-poor halo stars (MPHSs), when the lifetime of the unstable particles is of the order ~10^8–10^{12} s and their initial abundance with respect to that of the photons is ~$(10^{-13}$–10^{-12} GeV$)/E_{\gamma 0}$, where $E_{\gamma 0}$ is the emitted photon energy in the radiative decay. We conclude that the most likely nucleosynthetic scenario involves two different processes. First, a nonthermal cosmological nucleosynthesis associated with the radiative decay of unstable particles; and second, the stellar depletion of both of the primordial lithium isotopic abundances.

I. INTRODUCTION

In standard cosmology, the universe is thought to have experienced big bang nucleosynthesis (BBN) at a very early stage. D, T, ^{3}He, ^{4}He, ^{6}Li, ^{7}Li and ^{7}Be are produced appreciably at this epoch. Different types of observations have been made for the purpose of determining the primordial elemental abundances. These observational results provide rich information about the cosmic chemical evolution of the light nuclear species. Today BBN provides a very precise tool for inferring the condition of the early universe. BBN in the standard cosmology explains relatively well the inferred primordial abundances for a narrow range of the universal baryon-to-photon ratio η.

The Wilkinson Microwave Anisotropy Probe (WMAP) satellite has measured the temperature fluctuations of the cosmic microwave background (CMB) radiation, and parameters characterizing the standard big bang cosmology have been deduced [1,2] from these data. For the baryon-to-photon ratio η deduced from fits to the CMB, the BBN model predicts abundances of the light elements which are more-or-less consistent with those inferred from astro-nomical observations. This near agreement places significant limits on nonstandard models which influence the cosmic nuclear abundances.

In this regard, unstable massive particles decaying during or after the BBN epoch are strongly constrained [3–6]. For example, radiative decay [7–9], hadronic decay, or annihilation [10–12] have been studied recently, and several critical constraints on the relic particle properties were derived. These particle processes induce electromagnetic and/or hadronic showers which lead to the destruction of preexisting nuclei and to the production of different nuclear species. In turn, these modifications to the light-element abundances are used to constrain theories for the decay of relic particles. The physics associated with the general decay process (including a hadronic decay component) is explained in [12,13].

Superweakly interacting massive particles (SWIMPs) have been proposed [14] as candidates for cosmological dark matter. They are a form of nonbaryonic dark matter derived from theories beyond the standard model (SM) such as supersymmetry or universal extra dimensions (UED) [15]. The stable particles in these theories may constitute the dark matter, while the unstable particles could decay to modify the nuclear abundances in the early universe. This type of dark-matter particle interacts super-weakly with the SM fields and cannot be detected directly in experiments searching for conventional WIMPs. Thus,

*Electronic address: kusakabe@th.nao.ac.jp;
Research Fellow of the Japan Society for the Promotion of Science.

further studies of decay-induced nucleosynthesis could help to constrain such new particle theories.

Spectroscopic lithium abundances have been detected in the atmospheres of metal-poor stars. Nearly constant abundances of ^{6}Li and ^{7}Li in metal-poor Population II (Pop II) stars have been inferred [16–18]. Spectroscopic measurements obtained with high resolution indicate that metal-poor halo stars (MPHSs) have a very large abundance of ^{6}Li, i.e. at a level of about a twentieth that of ^{7}Li. This is about 3 orders of magnitude larger than the SBBN prediction of the ^{6}Li abundance.

It was suggested some time ago [5] that a high ^{6}Li abundance could be produced via particle decay. More recently, radiative particle decay, in particular, has been proposed [7] as the source of the abundant ^{6}Li observed in low metallicity stars. Furthermore, it was suggested [10] that hadronic decays which occur at around 1000 seconds after the big bang could simultaneously resolve both the ^{6}Li and ^{7}Li abundance issues. This probability has been studied within the context of supersymmetry, and there is sufficient parameter space for this to be possible [19]. A previous study on the radiative decay, however, was unable to provide a thorough solution to the lithium abundance puzzle [20]. In this paper, therefore, we consider this issue to be as of yet unresolved. We independently calculate the nucleosynthesis triggered by the radiative decay processes of long-lived relic particles over a wide range of parameters specifying the properties of the relic particles. We take into account the primary, secondary, and tertiary processes resulting from the electromagnetic cascade showers which both produce and destroy the light elements. We then constrain the abundance of long-lived particles from the calculated nucleosynthesis. We do not find, however, a simultaneous solution to both the ^{7}Li and ^{6}Li abundances unless there is stellar destruction of lithium.

This paper consists of the following structure. In Sec. II we describe briefly the formulae of nonthermal nucleosynthesis including the relevant photo-dissociation and nucleus-nucleus collisions. In Sec. III we summarize the observed light-element abundances and the constraints adopted in this work. The calculated results are shown in Sec. IV, where we derive the constraints on the parameters of decaying particles. In Sec. V, the constraints from the CMB spectrum are imposed, and the effects on small-scale structure are analyzed. The most interesting parameter region is deduced by taking the observational constraints on the light-element abundances into account. We conclude that our model can explain the desired ^{6}Li production by nonthermal nucleosynthesis even if there is stellar destruction of both lithium isotopes to explain the observed ^{7}Li.

II. MODEL

We assume the creation of high energy photons from the radiative decay of a massive particle with a lifetime of 10^2–10^{12} s. In this section we describe equations to calculate the nonthermal nucleosynthesis triggered by the appearances of high energy photons from decay. See [9] for details on the formulation which we adopt.

A. Initial nonthermal photon spectrum

We assume that the decaying dark particle is nonrelativistic, and almost at rest in the expanding universe. We denote the imaginary particle by X, [e.g. corresponding to the next-to-lightest supersymmetric particle (NLSP)] with a mass M_X that decays into a photon plus another dark-matter particle, [e.g. the lightest supersymmetric particle (LSP)]. We represent the emitted photon energy by $E_{\gamma 0}$.

When an energetic photon emerges, it interacts with the cosmic background and induces an electromagnetic cascade shower. The faster processes are pair production through background photons $\gamma \gamma_{\rm bg} (\gamma \gamma_{\rm bg} \to e^+ e^-)$ and inverse Compton scattering of produced electrons and positrons through background photons ($e^{\pm} \gamma_{\rm bg} \to e^{\pm} \gamma$). These two processes produce electromagnetic showers and the nonthermal photon spectrum realizes a quasistatic equilibrium [21,22]. The attained zeroth-generation photon spectrum can be written [23],

$$p_\gamma(E_\gamma) \approx \begin{cases} K_0 (E_X/E_\gamma)^{1.5} & \text{for } E_\gamma < E_X \\ K_0 (E_X/E_\gamma)^{2.0} & \text{for } E_X \le E_\gamma < E_C, \\ 0 & \text{for } E_C \le E_\gamma \end{cases} \quad (1)$$

where $K_0 = E_{\gamma 0}/(E_X^2[2 + \ln(E_C/E_X)])$ is a normalization constant fixed by energy conservation of the injected photon energy. This spectrum has a break in the power law at $E_\gamma = E_X$ and an upper cutoff at $E_\gamma = E_C$. We take the same energy scaling with the temperature T of the background photons as in [21], i.e. $E_X = m_e^2/80T$ and $E_C = m_e^2/22T$, where the cascade spectrum was calculated by numerically solving a set of Boltzmann equations.

Above $E_C = m_e^2/22T$, the rapid interaction between photons and electrons or positrons causes almost all energetic photons to quickly lose their energy. This leaves effectively no number spectrum for energies $E_\gamma > E_C$. In the context of the theory of electromagnetic cascade showers [23], the scale $E_X = m_e^2/80T$ corresponds to the point where the energy of the energetic photon is below the threshold for double photon pair creation. Hence, pair creation from interactions between energetic photons and the cosmic background radiation (CBR) ceases to operate.

The zeroth-generation nonthermal photons experience additional processes including: Compton scattering ($\gamma e_{\rm bg}^{\pm} \to \gamma e^{\pm}$); Bethe-Heitler ordinary pair creation in nuclei ($\gamma N_{\rm bg} \to e^+ e^- N$); and double photon scattering ($\gamma \gamma_{\rm bg} \to \gamma \gamma$). These slower processes further degrade the quasistatic equilibrium photon spectrum.

Because the rates of these electromagnetic interactions are faster than the cosmic expansion rate, the photon

spectrum is modified into a new quasistatic equilibrium (QSE). This distribution is given by

$$\mathcal{N}_\gamma^{\text{QSE}}(E_\gamma) = \frac{n_X p_\gamma(E_\gamma)}{\Gamma_\gamma(E_\gamma)\tau_X},\qquad(2)$$

where $n_X = n_X^0(1 + z)^3 \exp(-t/\tau_X)$ is the number density of the decaying particles at a redshift z, and τ_X is its mean life. The quantity Γ_γ is the energy degradation rate through the three slower processes for the zeroth-generation photons. We use this steady state approximation for the cosmic nonthermal constituent of photons. The Boltzmann equation describing the electromagnetic cascade processes is compiled in [21]. We used their relevant reaction rates to compute the cascade shower.

Because the cutoff scale of the photon energy is inversely proportional to the background temperature T, the cutoff scale comes to large as the universe cools. As a result, the number of the energetic nonthermal photons increases at low T.

B. Primary nucleosynthesis

The equation for the production and destruction of nuclei by nonthermal photons is given by

$$\frac{dY_A}{dt} = \sum_T \frac{N_A(T)}{N_T(T)!} Y_T \int_0^\infty dE_\gamma \mathcal{N}_\gamma^{\text{QSE}}(E_\gamma)\sigma_{\gamma+T\to A}(E_\gamma)$$
$$- Y_A \sum_P \frac{N_A(P)}{N_A(P)!} \int_0^\infty dE_\gamma \mathcal{N}_\gamma^{\text{QSE}}(E_\gamma)\sigma_{\gamma+A\to P}(E_\gamma),$$
$$(3)$$

where $Y_i \equiv n_i/n_B$ is the mole fraction of a particular nuclear species i, and n_i and n_B are number densities of nuclei i and baryons. The first and second term on the right-hand side are the source and sink terms for nucleus A. The source term includes the creation of nuclide A from all possible target nuclides T through a nonthermal photo-dissociation reaction $\gamma + T \to A$. And the sink term includes the destruction of nuclide A that is specified by the reaction $\gamma + A \to P$ for any produced nuclides P. E_γ is a nonthermal photon energy. The cross sections of processes $\gamma + T \to A$ and $\gamma + A \to P$ are denoted by $\sigma_{\gamma+T\to A}(E_\gamma)$ and $\sigma_{\gamma+A\to P}(E_\gamma)$. Further we use $N_K(L)$ to represent the number of a particular particle K relevant to a process $\gamma + a \to b$, where K is either a or b and L is T or P. For example, in the process $^4\text{He}(\gamma, d)d$, $N_d(^4\text{He}) = 2$ because two deuterons are produced from ^4He.

Next, we formulate the rate equation. We define $r \equiv n_X^0/n_\gamma^0$ and $H_r \equiv \sqrt{8\pi G \rho_{\text{rad}}^0/3}$, where the superscript 0 denotes present values ($z = 0$), therefore n_γ^0 and ρ_{rad}^0 are the present CBR photon number density and present radiation energy density, respectively. Then $n_X = n_X^0(1 + z)^3 \times \exp(-t/\tau_X)$ is transformed into $n_X = n_X^0(1/(2H_r t))^{3/2} \times \exp(-t/\tau_X)$, so that the rate Eq. (3) becomes

$$\frac{dY_A}{dt} = \sum_P N_A(P)\left(-\frac{Y_A}{N_A(P)!}[A\gamma]_P + \frac{Y_P}{N_P(P)!}[P\gamma]_A\right),$$
$$(4)$$

where we have defined the reaction rate

$$[B\gamma]_C = \frac{n_\gamma^0 \zeta_X}{\tau_X}\left(\frac{1}{2H_r t}\right)^{3/2}\exp(-t/\tau_X)$$
$$\times \int_0^\infty dE_\gamma\left(\frac{\tau_X}{E_{\gamma 0}n_X}\mathcal{N}_\gamma^{\text{QSE}}(E_\gamma)\right)\sigma_{\gamma+B\to C}(E_\gamma),$$
$$(5)$$

where $\zeta_X = rE_{\gamma 0}$.

The primary reactions and their cross sections are taken from [9].

C. Secondary nucleosynthesis

If the photo-dissociated light nucleus of a primary reaction has enough energy to induce further nuclear reactions, then secondary or tertiary processes are possible.

The equation describing the secondary production and destruction is obtained by taking into account the energy loss of nuclear species while propagating through the background. In most situations, the energy loss rate is faster than any sink of primary nuclei [9] so that they can be ignored in the evolution of the primary particles. However, for unstable particles, the sink terms must be evaluated. In general, because of the high reaction rate, the primary particles establish a quasistatic equilibrium. The abundance evolution is then represented by

$$\frac{dY_S}{dt} = \frac{N_A(A)}{N_T(A)!}\frac{N_S(S)}{N_A(S)!}\sum_{T,T'} Y_T Y_{T'}[TT']_S - (\text{sink term}),$$
$$(6)$$

where $N_K(L)$ has the same meaning as above. The quantity $[TT']_S$ is given by,

$$[TT']_S = \frac{\eta(n_\gamma^0)^2 \zeta_X}{\tau_X}\left(\frac{1}{2H_r t}\right)^3\exp(-t/\tau_X)$$
$$\times \int_0^\infty dE_A \frac{\sigma_{A+T'\to S}(E_A)\beta_A}{b_A(E_A)}$$
$$\times \int_{\mathcal{E}_A^{-1}(E_A)}^\infty dE_\gamma\left(\frac{\tau_X}{E_{\gamma 0}n_X}\mathcal{N}_\gamma^{\text{QSE}}(E_\gamma)\right)\sigma_{\gamma+T\to A}(E_\gamma)$$
$$\times \exp\left[-\int_{E_A}^{\mathcal{E}_A(E_\gamma)} dE_A'' \frac{\Gamma_A(E_A'')}{b_A(E_A'')}\right].$$
$$(7)$$

This is the reaction rate for a secondary process $T(\gamma, X_1)A(T', X_2)S$ with any combination of particles X_1, A, and X_2. The quantity η is the baryon-to-photon ratio: $\eta \equiv n_B^0/n_\gamma^0$, and β_A is the velocity of the primary particle A. $b_A = -dE/dt$ is the rate of energy loss of the primary particle. The energy loss rates are taken from [12]. Coulomb scattering ($Ne_{\text{bg}}^\pm \to Ne^\pm$) is the dominant loss

process for primary nuclei N. Then Γ_A is the coefficient of the primary particle sink, and in the case of an unstable nuclide, its value is the decay rate. $\mathcal{E}_A(E_\gamma)$ is the energy of the nuclide A produced by the photo-dissociation process $\gamma + T \rightarrow A$, simultaneously $\mathcal{E}_A^{-1}(E_A)$ is the energy of the nonthermal photons which produce the primary species A with energy E_A.

To simplify Eq. (7) we define

$$S_\gamma^{\mathrm{QSE}}(E_\gamma) = \frac{\tau_X}{E_{\gamma 0} n_X} \mathcal{N}_\gamma^{\mathrm{QSE}}(E_\gamma), \qquad (8)$$

and

$$P(E_A, E_\gamma) = \exp\left[-\int_{E_A}^{\mathcal{E}_A(E_\gamma)} dE_A'' \frac{\Gamma_A(E_A'')}{b_A(E_A'')}\right]. \qquad (9)$$

Then we denote the factors preceding the first integral by an overall normalization B to obtain

$$[TT']_S = B \int_{E_{p,\mathrm{th}}}^{\mathcal{E}_A(E_C)} dE_A \frac{\sigma_{A+T'\rightarrow S}(E_A)\beta_A}{b_A(E_A)}$$
$$\times \int_{\mathcal{E}_A^{-1}(E_A)}^{E_C} dE_\gamma S_\gamma^{\mathrm{QSE}}(E_\gamma)\sigma_{\gamma+T\rightarrow A}(E_\gamma)P(E_A, E_\gamma),$$
$$(10)$$

where lower limit for the external integral is replaced with the threshold energy of primary nuclide for the secondary reaction $E_{p,\mathrm{th}}$. Since the photon spectrum includes few energetic photons above E_C, the upper limit for internal integral can be changed to E_C. $\mathcal{E}_A(E_\gamma)$ and $\mathcal{E}_A^{-1}(E_A)$ are derivable in the limit of low energy scattering, where the relevant nuclei are nonrelativistic. The adoption of this limit is reasonable because most of the reactions occur with low energy photons near threshold. Thus, the produced primary nuclei are mostly nonrelativistic.

If the primary product particles are further destroyed by interactions with background particles, this secondary destruction process can have a large contribution to nonthermal nucleosynthesis. Thus we also take into account the destruction of D, T, ^{3}He and ^{6}Li after primary production by abundant background nuclides. For the destruction processes d + p and ^{3}He + p, we used the cross sections from [24,25]. For the t(p,dp)n and t(p,p2n)p reactions, we used cross sections from the mirror nucleus reactions ^{3}He(p, dp)p and ^{3}He(p, 2pn)p, respectively. Although the cross sections of t + p and ^{3}He + p reactions are different because of the Coulomb interaction, these mirror nucleus reaction cross sections are almost identical [26]. We adopt the cross section for ^{6}Li(p, ^{3}He)^{4}He from [27].

It has been found that only ^{6}Li can be produced by secondary nonthermal nucleosynthesis at a much higher level than by the SBBN, while the production of other nuclei e.g. D, ^{7}Li and ^{7}Be are insignificant [7,9,12]. The relevant processes in the secondary nonthermal production of ^{6}Li involve interactions of background ^{4}He with primary tritium or ^{3}He particles. Threshold energies of the

^{4}He(t, n)^{6}Li and ^{4}He(^{3}He, p)^{6}Li reactions are 8.3870 MeV and 7.0477 MeV, respectively. We have taken into account these two reactions with their cross sections from [9].

The survival probability should also be considered in order to calculate the precise abundance [12]. This destruction of ^{6}Li is included in the SBBN code [12]. Therefore the formulation of the survival probability should not include the process after the thermalization of ^{6}Li to prevent a double counting of ^{6}Li destruction.

III. OBSERVATIONS OF LIGHT-ELEMENT ABUNDANCES

A. Light-element abundances

The primordial abundances of D, ^{3}He, ^{4}He, and ^{7}Li are inferred from various observations. Recently ^{6}Li has been measured for numerous old halo stars and a so-called ^{6}Li plateau as a function of metallicity appears to exist [28]. The reliability of inferred primordial abundances from several types of observations is difficult to estimate because of systematic errors. Here, we summarize the observational data and our adopted constraints.

Deuterium is measured in absorption spectra at high redshift toward QSOs. Since the ratio D/H is low, D can only be detected in absorption systems with high HI column densities. This causes a difficulty for such observations. From the Keck I HIRES spectra of Q1243 + 3047, a deuterium abundance of D/H = $2.42^{+0.35}_{-0.25} \times 10^{-5}$ is estimated [29]. The best estimate of the primordial D/H from absorption systems toward five QSOs reported in that paper, is

$$\mathrm{D/H} = 2.78^{+0.44}_{-0.38} \times 10^{-5}. \qquad (11)$$

However, the five values have a larger dispersion than that inferred from the individual measurements. Hence, the errors are probably underestimated. We therefore take the highest value of D/H in the five values, D/H = $3.98^{+0.59}_{-0.67} \times 10^{-5}$ and allow for a two sigma increase above this value to fix an upper limit. In the standard theory of galactic chemical evolution, deuterium continually decreases in time by the processing of interstellar material through stars. Hence, we take the present abundance of deuterium as the lower limit. Column densities of DI along seven lines of sight have been estimated from observations with the Far Ultraviolet Spectroscopic Explorer (FUSE), and the local interstellar medium at a distance of 37–179 pc has been probed [30]. The weighted mean value of DI/HI for five data, with reliable values for column densities of HI determined, is $(1.52 \pm 0.08) \times 10^{-5}$. When we allow for a two sigma lower limit, we get the following constraint on the primordial abundance of deuterium

$$1.4 \times 10^{-5} < \mathrm{D/H} < 5.2 \times 10^{-5}. \qquad (12)$$

^{3}He is measured in Galactic HII regions by the 8.665 GHz (3.46 cm) hyperfine transition of ^{3}He$^+$ [31]. A plateau with a relatively large dispersion with respect to metallicity has been found at a level of ^{3}He/H $= (1.9 \pm 0.6) \times 10^{-5}$. There is a problem, however. Although stars are thought to produce ^{3}He, and ^{3}He enhancement is observed in planetary nebulae, the chemical evolution of ^{3}He has not been detected in the Galaxy during the last 4.5 Gyr [32,33]. This fact has recently been confirmed by more precise determination of the helium isotopic composition of the local interstellar cloud [34]. It is not yet understood, therefore, whether ^{3}He has increased or decreased through the course of stellar and galactic chemical evolution [35,36]. Thus, we adopt the two sigma upper limit from Galactic HII region abundances, that is

$$^3\text{He/H} < 3.1 \times 10^{-5}. \qquad (13)$$

We will discuss later an implication for a tighter constraint as suggested in [34], i.e. ^{3}He/H $< (1.6 \pm 0.3) \times 10^{-5}$, too. We do not give a lower limit due to the large uncertainty in the galactic production of ^{3}He.

^{4}He is measured in the HII regions of metal-poor external galaxies where chemical evolution is thought to be minimal. The primordial abundance is estimated to be $Y = 0.2421 \pm 0.0021$ by extrapolating the abundance to zero metallicity (O/H $= 0$) [37]. However, in [38] it is noted that there are sources of systematic uncertainty in determinations of the ^{4}He abundance. They suggest somewhat larger error bars with an abundance of $Y = 0.249 \pm 0.009$. They thus adopt a primordial ^{4}He abundance within the conservative range of

$$0.232 < Y < 0.258. \qquad (14)$$

We also adopt this constraint for the primordial ^{4}He abundance.

^{7}Li is measured in metal-poor halo stars (MPHSs) by the spectra of their atmosphere. There is about a factor of 3 under-abundance of ^{7}Li in MPHSs with respect to the SBBN prediction when using the baryon-to-photon ratio η inferred from the analysis of the CMB anisotropy. This is called the lithium problem [16,17,28]. For a recent review of the lithium problem, see [39], where possible resolutions of this problem are discussed.

Recently, high quality spectra for 24 metal-poor halo dwarfs and subgiants have been obtained [28]. They estimated a mean ^{7}Li abundance of $\log\epsilon_{^7\text{Li}} = 2.21 \pm 0.07$. Different groups derive somewhat different values. We adopt the estimate of [28] for the primordial ^{7}Li abundance allowing for a two sigma range, $\log\epsilon_{^7\text{Li}} = 2.07 - 2.35$ or

$$1.17 \times 10^{-10} < {}^7\text{Li/H} < 2.23 \times 10^{-10}. \qquad (15)$$

In addition, we take into account the possibility of the stellar depletion of lithium up to 0.5 dex to derive an upper limit to the primordial abundance,

$$1.1 \times 10^{-10} < {}^7\text{Li/H} < 7.1 \times 10^{-10}. \qquad (16)$$

As for the depletion of lithium in halo stars, it has been reported [40] that the mean lithium abundance and its dispersion appear to be lower for dwarf stars than for turn-off and subgiants. ^{7}Li abundances of 28 such halo subgiants have been measured [41]. The result is that (excluding the extremely lithium-rich subgiant BD + 233912) the maximum abundance is $\log\epsilon_{^7\text{Li}} = 2.35$. This is well below the SBBN predicted value. A calculation of the stellar depletion of lithium isotopes by atomic and turbulent diffusion leads [42] to an abundance reduction by a factor of at least 1.6–2.0 of the ^{7}Li abundance for Population II stars with metallicity [Fe/H] ≤ -1.5.

^{6}Li has also been measured in MPHSs by spectroscopy. In [28], ^{6}Li was detected at a better than two sigma significance in nine of the 24 stars observed. They suggest that a ^{6}Li plateau exists at $\log\epsilon_{^6\text{Li}} \approx 0.8$. This plateau implies important information because the SBBN would predict that much less primordial ^{6}Li be formed (^{6}Li/^{7}Li $\sim 10^{-5}$). Therefore, some mechanism should have produced almost all ^{6}Li in MPHSs. There are several candidates. For example, gravitational shocks during the hierarchical structure formation of the Galaxy could have accelerated cosmic rays (CRs) and produced ^{6}Li by $\alpha - \alpha$ fusion reactions at a very early stage [43,44]. A scenario has also been suggested [18,45] whereby cosmological CRs (perhaps related to pop III stars) were produced at an extremely early epoch up to the formation of the Galaxy. These CRs could then have produced ^{6}Li by $\alpha + \alpha$ fusion. See the discussion in [46] for a recent summary of various candidates for ^{6}Li production. Another new mechanism has been proposed recently [47] whereby ^{6}Li originated from the binding of negatively charged particles to background nuclei. Since multiple processes have possibly synthesized ^{6}Li at an early epoch, we do not put limits on the primordial abundance of ^{6}Li. However, we adopt the average value of the abundance derived from the eight MPHSs with detections as a guide to constrain possible production from radiative decay,

$$^6\text{Li/H} \approx 6.6 \times 10^{-12}. \qquad (17)$$

B. Cosmic microwave background anisotropy

Very precise data have been obtained by observations of the spectrum of temperature fluctuations in the CMB. The WMAP data have been analyzed and the energy density of baryons in the universe has been deduced along with other cosmological parameters. This leads to $\Omega_b h^2 = 0.0224 \pm 0.0009$ for the WMAP first year data [1] and $\Omega_b h^2 = 0.0207^{+0.0008}_{-0.0011}$ for the WMAP 3 yr data [2] in the running scalar spectral index model. We adopt the first year result, corresponding to $\eta = (6.1^{+0.3}_{-0.2}) \times 10^{-10}$. The SBBN with the WMAP $\Omega_b h^2$ parameter region has been calculated including the uncertainties of the inferred $\Omega_b h^2$ and the

reaction rate uncertainties on the SBBN [48]. Their result is

$$D/H = (2.60^{+0.19}_{-0.17}) \times 10^{-5}, \qquad (18)$$

$$^3He/H = (1.04 \pm 0.04) \times 10^{-5}, \qquad (19)$$

$$Y = 0.2479 \pm 0.0004, \qquad (20)$$

$$^7Li/H = (4.15^{+0.49}_{-0.45}) \times 10^{-10}. \qquad (21)$$

IV. RESULTS

We have calculated the cosmological nucleosynthesis including the SBBN and nonthermal nucleosynthesis induced by the radiative decay of a long-lived massive particle. The SBBN was computed using the Kawano code [49] with the use of the new world average of the neutron lifetime [50]. We added the nonthermal components of Eq. (4) and (6) also taking into account the destruction of secondarily produced ^6Li. We deduced properties of the decaying particle in terms of its lifetime τ_X and abundance ζ_X with the baryon-to-photon ratio fixed at $\eta = 6.1 \times 10^{-10}$. We checked the effect of secondary destruction of the primary nonthermal nuclides. We confirmed that the energy loss is much faster than the destruction (see the discussion for nonthermal ^6Li production of [9]). The secondary destruction processes of primary nuclides were not very efficient (destruction probabilities are $\leq \mathcal{O}(10^{-3})$). The final abundances were therefore not much affected by secondary destruction.

The point is that the time scale of the Coulomb loss for the nonthermal nuclides is much smaller than those of the destruction reactions at low energies. Furthermore, the destruction probabilities of nonthermally produced ^6Li are very small, and produced ^6Li survives [12].

We have derived the constraints on the lifetime τ_X and abundance parameter ζ_X from the adopted limits for the cosmological light-element abundances. Our result is very similar to that of [9], since we use the same formulation for nonthermal nucleosynthesis and adopt their fitted cross sections. A detailed explanation has been given in [9] for the systematics of the radiative decay.

Figure 1 shows a contour of the ^4He mass fraction $Y > 0.232$ (red line) in the (τ_X, ζ_X) plane. Above this contour, $Y < 0.232$. Since ^7Li is more weakly bound than ^4He, the destruction happens even in shorter lifetime conditions. The contour of ^7Li for the lower limit of $^7Li/H > 1.1 \times 10^{-10}$ (blue line) has the shape plotted on Fig. 1. Contours for D/H upper and lower limits, $D/H \leq 5.2 \times 10^{-5}$ (green solid lines) and $D/H \geq 1.4 \times 10^{-5}$ (green dashed lines), respectively, are also shown. Contours for the $^3He/H$ upper limit, $^3He/H \leq 3.1 \times 10^{-5}$ (black lines) are also drawn. The shape of this contour is very analogous to that for the D/H upper limit. This reflects the fact that the photodisin-
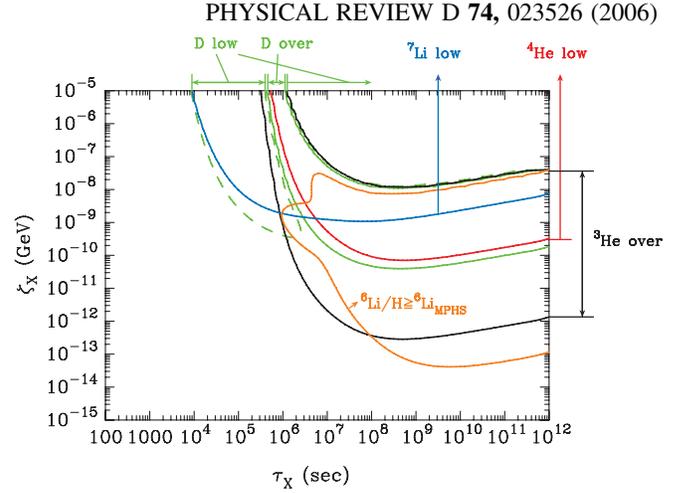

FIG. 1 (color). Contours in the (τ_X, ζ_X) plane corresponding to the adopted constraints for the primordial abundances in models with a fixed value of $\eta = 6.1 \times 10^{-10}$. Contours for the mass fraction of ^4He $Y = 0.232$ (red line) and the number ratios of $^3He/H = 3.1 \times 10^{-5}$ (black lines), $D/H = 5.2 \times 10^{-5}$ (green solid lines), $D/H = 1.4 \times 10^{-5}$ (green dashed lines), and $^7Li/H = 1.1 \times 10^{-10}$ (blue line) are shown. The contour of $^6Li/H = 6.6 \times 10^{-12}$ (orange line) is also drawn. The notation "over" and "low" identifies overproduced and underproduced regions, respectively.

tegration of ^4He is the main cause of the production of both D and ^3He. Finally, the contour for the MPHSs level of $^6Li/H = 6.6 \times 10^{-12}$ is plotted to see the behavior of the ^6Li nonthermal production (orange line).

Figure 2 shows the derived constraint on τ_X and ζ_X for an unstable particle from the consideration of the light-element abundances above described in a model with $\eta = 6.1 \times 10^{-10}$. All limits from the light-element abundances
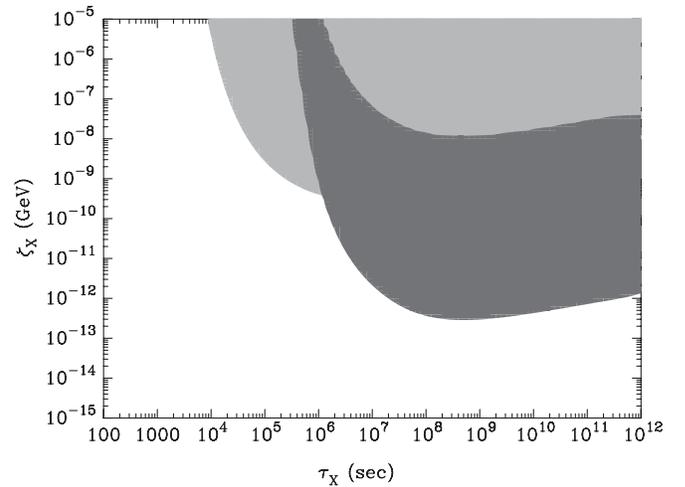

FIG. 2. Colored regions identify the excluded area in the parameter space (τ_X, ζ_X) for models with a fixed value of $\eta = 6.1 \times 10^{-10}$. The dark shaded region is excluded by an over-abundance of ^3He, whereas the light shaded region is mostly excluded by an under-abundance of deuterium.

used in this study, for D/H, ^{3}He/H, Y and ^{7}Li/H have been taken into account. The ^{3}He overabundant region is shaded by the dark color, and the rest of the excluded region the light color. The light colored region is fixed largely by the deuterium underproduction. For $\tau_X \gtrsim 10^6$ s, ^{3}He provides the strongest limit on the abundance parameter yielding,

$$\zeta_X \leq 4 \times 10^{-13} \text{ GeV},\tag{22}$$

while for shorter lifetimes ($\tau_X \sim 10^4$–10^6 s) the limits are from D implying $\zeta_X \lesssim 10^{-9}$ GeV.

Uncertainties from the reaction cross sections have been discussed in [9]. The uncertainties from the photo dissociation and secondary cross sections are of the order of 10%. In addition, we confirmed that effects of errors in the cross sections for the secondary destruction reactions are negligible. The BBN light-element abundances are then the dominant source of uncertainty. The BBN cross section uncertainties are not included in our study, but they are estimated [e.g. Eq. (18)–(21)], and one can apply those to our nonthermal calculation results.

V. DISCUSSION

A. Distortion of the CMB spectrum

The abundance of massive decaying particles is also constrained from the observed spectrum of CMB radiation. Since nonthermal photons produced by the radiative decay deform the black-body spectrum of the CMB, this is limited by the consistency of the observed CMB data with a black-body spectrum [14,51]. For epochs earlier than $z \sim 10^7$, thermal bremsstrahlung, [i.e. free-free emission ($eN \rightarrow eN\gamma$), where N is an ion] and radiative-Compton scattering ($e^-\gamma \rightarrow e^-\gamma\gamma$) act effectively to erase any distortion of the CBR spectrum from a black body. For the decay in epochs $10^5 < z < 10^7$, processes changing the photon number become ineffective, and Compton scattering ($\gamma e^- \rightarrow \gamma e^-$) causes the photons and electrons to achieve statistical equilibrium, but not thermodynamic equilibrium. Then, the photon spectrum should have a Bose-Einstein distribution

$$f_\gamma(\vec{p}_\gamma) = \frac{1}{e^{\epsilon_\gamma/T+\mu} - 1},\tag{23}$$

where μ is the usual dimensionless chemical potential derived from the conservation of photon number.

Analyses of the CMB data suggest a relatively low baryon density so that double Compton scattering dominates the thermalization process. For small energy injection from the radiative decay, the chemical potential can be approximated analytically [51,52] as

$$\mu = 4.0 \times 10^{-4} \left[\frac{\tau_X}{10^6 \text{ s}}\right]^{1/2} \left[\frac{\zeta_X}{10^{-9} \text{ GeV}}\right] e^{-(\tau_{\text{dC}}/\tau_X)^{5/4}},\tag{24}$$

where

$$\tau_{\text{dC}} = 6.1 \times 10^6 \text{ s}\left[\frac{T_0}{2.725 \text{ K}}\right]^{-12/5} \left[\frac{\Omega_b h^2}{0.022}\right]^{4/5}$$
$$\times \left[\frac{1 - Y/2}{0.88}\right]^{4/5},\tag{25}$$

where T_0 is the present CMB temperature, and $h = H_0/(100 \text{ km s}^{-1} \text{ Mpc}^{-1})$ is the normalized Hubble parameter.

For a late energy injection at $z < 10^5$, Compton scattering produces little effect and cannot establish a Bose-Einstein spectrum. The distorted spectrum is then described by the Compton y parameter. There is a relation between y and the amount of the injected energy, $\Delta E/E_{\text{CBR}} = 4y$, where ΔE and E_{CBR} are the total energy injected and the CBR energy, respectively. The ratio of the energy injected by radiative decay to the CBR energy per comoving volume can be expressed as

$$\frac{\Delta E}{E_{\text{CBR}}} = \frac{E_{\gamma 0}}{2.7T(t_{\text{eff}})}\left[\frac{n_{X0}}{n_{\gamma 0}}\right] = \frac{\zeta_X}{2.7T(t_{\text{eff}})},\tag{26}$$

where $t_{\text{eff}} = [\Gamma(1 + \beta)]^{1/\beta}\tau_X$ for $T \propto t^{-\beta}$, with $\Gamma(x)$ the gamma function of argument x. The factor of 2.7 comes from the fact that the average energy of the CBR photons at a given temperature is $2.7T$. The time-temperature relation is $T \propto t^{-1/2}$ for a radiation dominated universe.

The CMB spectrum has been well measured and the deduced limits are $|\mu| < 9 \times 10^{-5}$, $|y| < 1.2 \times 10^{-5}$ [53] and $\Omega_b h^2 \sim 0.022$ with $h \sim 0.71$ [1]. Therefore, the high abundance parameter region of ζ_X is excluded by the μ and y limits. In Fig. 3 the black shading indicates the parameter region excluded by the CBR distortion limit. For a lifetime shorter than $\tau_X = 4 \times 10^{11}$ s $\Omega_b h^2 \sim 8.8 \times 10^9$ s, the decay is constrained by the chemical potential μ. On the other hand, when an unstable particle decays later, the CBR spectrum is limited by the Compton y parameter. The parameter region of relatively long lifetime (10^{10} s $< \tau_X$) is found to be constrained by the CMB spectrum more strongly than the light-element abundances.

The discussion so far has assumed that η at the BBN epoch can be determined from the power spectrum of CMB temperature fluctuations. However, η could have changed from the BBN epoch to the time of the recombination [54]. The entropy production resulting from the photon emission by radiative decay has been estimated and it is very small for a large part of the region allowed by the nonthermal nucleosynthesis and CMB distortion constraints in Fig. 3. However, for very early decay ($\tau_X < 10^4$ s) entropy production could be large. An entropy change by as large as $\Delta S/S_i \sim 10^{-1}$ seems unlikely since the CMB-favored value of $\eta = 6.1 \times 10^{-10}$ is transformed into 6.7×10^{-10} at the BBN epoch and this would bring about a more severe discrepancy of the ^{7}Li abundances between the SBBN prediction including the nonthermal processes and estimations from the MPHSs observations. See Fig. 3 in [54]
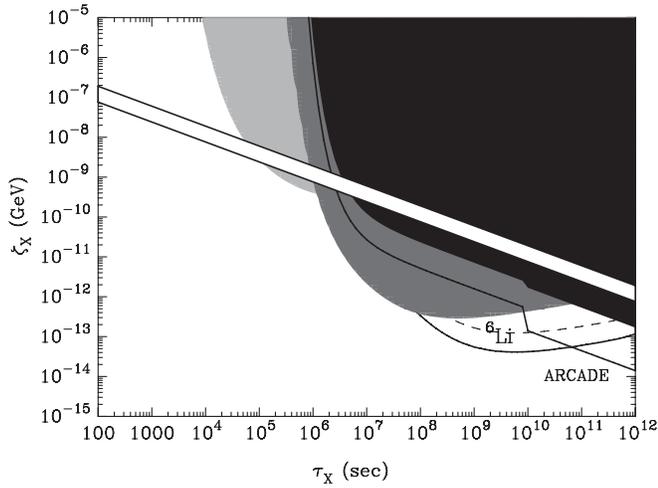
FIG. 3. Same as in Fig. 2 except that the black shaded region is superimposed. This region shows the region excluded by the consistency requirement of the CMB with a black-body. The white band identifies parameter values where the free-streaming of decay products would lead to a suppression of small-scale structure growth in a model with $\Omega_Y h^2 \sim 0.11$. The curved line identifies the contour of $^6\text{Li}/\text{H} = 6.6 \times 10^{-12}$, corresponding to the abundance of ^6Li observed in MPHSs. The region above the contour and below the nucleosynthesis and CMB constraints is allowed and abundant in ^6Li. The contour for ^6Li enhanced by 3 times as much MPHSs value is also drawn (dashed line). The solid line corresponds to the sensitivity of the planned ARCADE mission as labeled.

B. Effects on small-scale structure

The decay products obtain momentum from the decay by simple momentum conservation. This momentum can affect structure formation in the universe. In this regard there are useful constraints on the present root-mean-square velocity of warm dark matter from observations of the Lyman-α forest [55] and supermassive black holes at high redshift [56]. Limits from the early reionization have also been reported [56,57]. The free-streaming decay products must not cause an inconsistency with observations. This consideration of free-streaming has been discussed in detail in [19].

Cold, collisionless, non-self-interacting dark matter explains the trend of the observed structures larger than ~ 1 Mpc. However, it does not successfully explain the structure at smaller scales. As a solution to the small-scale structure problem, the decay of SWIMPs has been proposed [58]. The velocity dispersion reduces the 6-dimensional phase space density and prevents the formations of cuspy halos. Furthermore, the free-streaming of dark-matter particles damps the power spectrum at small scales. They discuss the paradigm in which the dark matter is composed mostly of the decay products. In this case the parameters which lead to reasonable free-streaming predict roughly the correct phase space density. Therefore we only discuss the free-streaming scale.

If the free-streaming scale is reasonably small ~ 1 Mpc, the free-streaming scale λ_{FS} from the decay time to the present ($z \sim 0$) is described [58] as

$$\lambda_{\text{FS}} \approx 1.5 \text{ Mpc } u_Y \left[\frac{\tau_X}{10^6 \text{ s}} \right]^{1/2}, \tag{27}$$

where $u_Y \equiv p_Y/m$ is momentum at the decay time divided by the mass of the particle Y produced by the decay. In the range of $\tau_X \lesssim 10^{12}$ s, this approximation involves a maximum error of only a factor 1.5 in the numerical factor. The largest error comes when $\tau_X = 10^{12}$ s and correspondingly $u_Y \sim 10^{-3}$. From momentum conservation during the decay, the momentum of product p_Y is equal to the emitted photon energy $E_{\gamma 0}$. The parameter ζ_X is written as

$$\zeta_X = 2.6 \times 10^{-8} \text{ GeV}(\Omega_Y h^2) u_Y, \tag{28}$$

where Ω_Y is the energy density normalized to the critical density.

Equations (27) and (28) connect the τ_X and ζ_X by the elimination of u_Y. Such decay can be a resolution to the small-scale structure problems if the free-streaming scale is $0.4 \text{ Mpc} \lesssim \lambda_{\text{FS}} \lesssim 1.0 \text{ Mpc}$ [58]. This limit determines the suitable parameter space for τ_X and ζ_X under the assumption of $\Omega_Y h^2 \sim 0.11$ [1]. This region is shown in Fig. 3 as a white band bounded by solid lines. The region above this band is excluded in this case, since the decay products erase the larger scale fluctuations. The region below this band will be discussed in the next subsection in connection with the ^6Li abundance. Apparently, the decay at $\tau_X \gtrsim 10^5$ s is not realistic because the effect on the light-element abundances or CBR spectrum is prohibitively large. On the other hand relatively early decay at $\tau_X \lesssim 10^5$ s is viable. Applying this result to a model for a gravitino SWIMP with a photino NLSP [58], we obtain $m_{\text{SWIMP}} \lesssim 200$ GeV and $\Delta m \sim 400$–700 GeV.

C. ^6Li-producing parameter region

In this paper we analyze the possibility that the radiative decay of long-lived particles produces ^6Li by nonthermal process while having almost no effect on ^7Li or other nuclides produced in the SBBN. Ellis, Olive & Vangioni researched the possibility that the radiative decay of unstable particles explains the discrepancy of the BBN calculated ^7Li abundance and low ^7Li plateau derived from observations [20]. They found that in the parameter region where ^7Li is photo-dissociated down to the level of the ^7Li plateau, either the D abundance was too low or the ratio $^3\text{He}/\text{D}$ was unacceptably large in the context of standard stellar evolution and chemical evolution. Consequently, they concluded that radiative particle decays cannot be a cause for the ^7Li abundance difference. They also mentioned the possibility of ^6Li production in their paper.

Uncertainties remain in estimations of the Li abundance in stellar atmospheres, and the probability of depletion in stars has not been excluded. The difference between abun-

dances determined by different analysis approaches is also a concern. Therefore, we suppose that the discrepancy of the ^{7}Li abundance is caused by stellar depletion or some other systematic effect. Then the ^{6}Li abundance in the early universe should have been larger when first engulfed in a star than the value presently deduced from observations of MPHSs. Assuming that is the case, we impose the following constraint on the ^{6}Li abundance after the radiative decay process,

$$^6\text{Li/H} > 6.6 \times 10^{-12}. \quad (29)$$

If this process is responsible for the high ^{6}Li abundance in MPHSs, this is the limit to be adopted. Although previous studies [7,20] give the ^{6}Li abundance of MPHSs as the upper limit, we adopt this as the lower limit considering the possibility of stellar destruction.

In Fig. 3 the contour of the lower limit (29) is shown by a solid line below the CMB constraint. Hence, a ^{6}Li-producing allowed parameter region certainly exists for $\tau_X = 10^8$–10^{12} s and $\zeta_X \sim 10^{-13}$–10^{-12} GeV. The parameter region allowed by the above constraints which also produces abundant ^{6}Li is marked as "^{6}Li."

This ^{6}Li-producing zone is somewhat close to the limit deduced by fits to the CMB distortion. Thus, future measurements of the CMB spectrum may reach this parameter region and provide better limits to this radiative decaying particle scenario. The absolute radiometer for cosmology, astrophysics, and diffuse emission (ARCADE) [59,60] will observe the CMB at centimeter wavelengths with better sensitivity than current data. ARCADE may make it possible to impose a limit on the chemical potential up to $|\mu| < 2 \times 10^{-5}$ and Compton y parameter up to $y < 10^{-6}$, respectively. This sensitivity corresponds to the solid line marked as "ARCADE" in Fig. 3. It spans the parameter region for producing 3 times as much ^{6}Li as MPHSs (a dashed line, see discussion below). Thus, if ARCADE does not detect the spectral distortion, ^{6}Li production from radiative decay can be ruled out.

The allowed parameter region has a very small entropy increase of less than the order of 10^{-5}, so that this has a negligible effect on the deduced η. We have analyzed this parameter region to see the possibility of realization. It is important to check the results of the nonthermal nucleosynthesis for decay in the ^{6}Li-producing region. We made a model calculation with input parameters of $\tau_X = 1 \times 10^{10}$ s, $\zeta_X = 3 \times 10^{-13}$ GeV and $\eta = 6.1 \times 10^{-10}$. The final abundances obtained in this model are

$$\text{D /H} = 2.63 \times 10^{-5}, \quad (30)$$

$$^3\text{He/H} = 2.48 \times 10^{-5}, \quad (31)$$

$$Y = 0.247, \quad (32)$$

$$^6\text{Li/H} = 4.69 \times 10^{-11}, \quad (33)$$

$$^7\text{Li/H} = 4.36 \times 10^{-10}. \quad (34)$$

These are certainly consistent with the constraints we adopted in Sec. III A. The abundances of ^{3}He and ^{6}Li with respect to the SBBN abundances increase. In fact, the nonthermal production of ^{6}Li is unavoidably accompanied by ^{3}He production. We confirmed that the produced amounts of ^{3}He and ^{6}Li are proportional to ζ_X when τ_X is fixed. However, for a longer decay lifetime, the ^{6}Li production is relatively more effective than the ^{3}He production because of the different dependences of the production rates on the CBR temperature.

If the inconsistency between the ^{7}Li abundance predicted by SBBN and that measured from MPHSs is caused by depletion, ^{6}Li would have existed in the primordial gas at a level larger than the abundance observed in MPHSs by at least the ratio of the SBBN ^{7}Li/H prediction to the mean value observed in MPHSs. The observed ^{7}Li/H abundance [28] is ^{7}Li/H $\sim 1.62 \times 10^{-10}$. Hence, this factor is about $(4.36 \times 10^{-10})/(1.62 \times 10^{-10}) \sim 3$. So ^{6}Li should have been originally produced at an abundance more than about 3 times the presently observed value. We stress that the nonthermal ^{6}Li production inevitably brings about the production of ^{3}He, and this gives a strong constraint on the possible parameter space of unstable particles [12,20].

We have analyzed the upper limit to the ^{6}Li abundance resulting from the radiative decay process under the requirement of consistency with the other light-element abundances. In Fig. 4, the ^{6}Li abundances are plotted as a function of τ_X. Points on this figure are allowed by the constraints imposed above and lead to ^{6}Li abundances

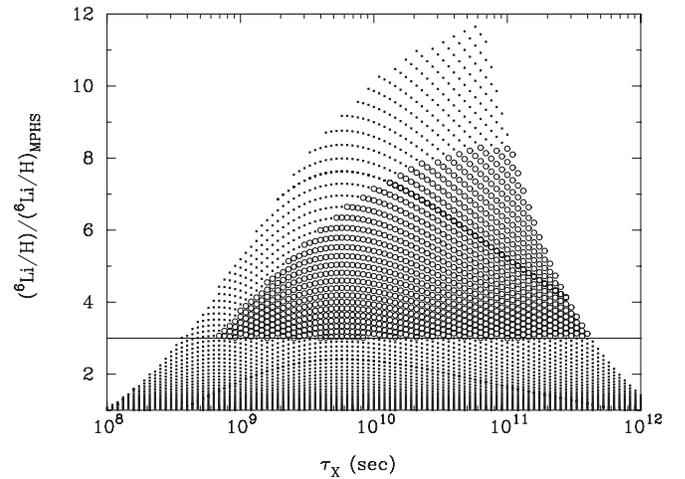FIG. 4. Ratio of calculated ^{6}Li/H abundances (after the nonthermal nucleosynthesis) to the observed abundance in MPHSs as a function of τ_X. Results in the allowed parameter region of (τ_X, ζ_X) producing ^{6}Li/H larger than the value found in MPHSs, or the marked region "^{6}Li" in Fig. 3 are plotted. The horizontal line indicates a factor of 3 overproduction of ^{6}Li relative to the observed MPHS value of ^{6}Li/H $= 3 \times 6.6 \times 10^{-12}$. The large circles denote values in the allowed region with abundances of ^{3}He/H $= 1.3$–2.5×10^{-5} and ^{6}Li/H $\geq 3 \times 6.6 \times 10^{-12}$. The other parameters sets are indicated by small squares.

above the level observed in MPHSs. The vertical scale is ^{6}Li/H normalized to the mean ^{6}Li/H abundance in MPHSs (^{6}Li/H)$_{\rm MPHS}$. The horizontal line indicates a factor of 3 enhancement in ^{6}Li. The large circles are for cases with more than 3 times as abundant ^{6}Li as the level found in MPHSs. Here, we adopt the one sigma ^{3}He/H $= (1.9 \pm 0.6) \times 10^{-5}$ [31] as an extra constraint. We note that, in cases adopting a tighter constraint ^{3}He/H $< (1.6 \pm 0.3) \times 10^{-5}$ [34], one can still find an allowed region of $\tau_X = 3 \times 10^{10}$–$3 \times 10^{11}$ s which satisfies the same constraint imposed on the ^{6}Li abundance. The small squares are for other cases of Eq. (13).

This figure confirms that ^{6}Li/H abundances as large as those in MPHSs multiplied by the ratio (^{7}Li/H)/ (^{7}Li/H)$_{\rm MPHS}$ can be produced by nonthermal nucleosynthesis without significantly impacting the other nuclide abundances. Although this explanation could resolve the discrepancy between the SBBN predicted ^{6}Li abundances and those derived from observations, it cannot resolve the lithium problem. This scenario necessarily requires some model for the stellar depletion of ^{6}Li and ^{7}Li. Indeed, as discussed in [28] and references therein, models exist which suggest a very large depletion factor of ^{6}Li along with some ^{7}Li depletion. The production of ^{6}Li by radiative decay cannot explain the observed abundances of both ^{6}Li and ^{7}Li, if the stellar depletion proceeds as described by that model. However, approximately equal amounts of depletion for both lithium isotopes can explain the measured abundances when combined with the nonthermal production of ^{6}Li. As for the case including the hadronic decay process [19], it has been found that such particle decay could simultaneously solve both the ^{6}Li and ^{7}Li problem, even if a possible degree of depletion is included. Clearly, further research on such depletion processes, along with analysis of more observational data, is desired.

VI. CONCLUSION

We have investigated the possibility that nonthermal nucleosynthesis induced by the radiative decay of long-lived particles contributed to the light-element abundances in the early universe. We have constrained this process by observed primordial light-element abundances. The primordial nucleosynthesis induced by high energy nonthermal photons from the radiative decay of long-lived relic particles was calculated taking into account both the primary nuclear production reactions and the effects of secondary production and destruction processes. We find, however, that the secondary destruction processes of primary D, T, ^{3}He and ^{6}Li have little influence on the final light-element abundances and, in particular, it is confirmed that the effect of the destruction of the produced ^{6}Li is very small in the cosmic temperature regime where the nonthermal secondary ^{6}Li production is operative.

We have utilized the observed light-element abundances from various sources to explore the constraints on the

parameter space of the lifetime (τ_X) and initial abundance (ζ_X) of unstable particles in a model in which the baryon-to-photon ratio η is fixed to the value inferred from the WMAP CMB power spectrum. We require that the nonthermal processes do not cause significant deviations from the observationally inferred primordial abundances. For each given lifetime τ_X we deduce an upper limit to the product ζ_X of the photon energy of the radiative decay and the fraction of the number density of the decaying particles to that of the CBR photons. For short lifetimes, $\tau_X < 10^6$ s, the lower limit to ζ_X is fixed by a D under-abundance, whereas for longer lifetimes, ^{3}He overproduction gives the strongest upper limit to ζ_X.

The parameter values are also constrained by the induced distortion of the CMB black-body spectrum from energetic photons emitted in the decay. The CMB constraint is more important than the light-element abundance constraints for the case of a long lifetime $\tau_X > 10^{10}$ s. Future missions such as ARCADE would, perhaps, detect the signal of the radiative decay. Otherwise, the production of ^{6}Li in this process is constrained.

Next we considered the free-streaming scale of the decay products. We imposed a constraint on the abundance parameter ζ_X under the assumption that the decay products comprise a dominant constituent of the cosmological dark matter. For the specific model of Ref. [58] a relatively late decay at $\tau_X > 10^5$ s is forbidden.

We studied the possibility of ^{6}Li production in nonthermal nucleosynthesis at a level which is comparable with the observed abundance in MPHSs. We find that there exists a parameter region leading to final abundances which are in reasonable agreement with the MPHS observations of ^{6}Li and is also consistent with the observational constraints on the other light nuclides. We show that if $\tau_X \sim 10^8$–10^{12} s and $\zeta_X \sim 10^{-13}$–10^{-12} GeV, it is possible that the radiative decay of long-lived relic particles causes the observed enhanced abundance of ^{6}Li in MPHSs.

Analyzing the results of the light-element abundances for the interesting particle parameter region in more detail, two important characteristics were found: One is that the excess ^{6}Li abundances from the nonthermal processes is regulated by the amount of ^{3}He coproduction because ^{3}He is the seed for ^{6}Li in the process ^{4}He(^{3}He, p)^{6}Li. Hence, the radiative decay model which results in ^{6}Li-production above the MPHS abundance level is also reflected by an enhancement of the ^{3}He abundance with respect to the SBBN value. Therefore, tighter constraints on the primordial ^{3}He abundance might exclude some parameter regions. However, a certain range of the possible parameter region still remains.

Another feature regarding this scenario of nonthermal ^{6}Li production triggered by the radiative decay is that it does not resolve the lithium problem. Other mechanisms such as the stellar depletion of the lithium isotopes must operate to lower the ^{7}Li abundance in the atmosphere of

MPHSs. In such mechanisms, however, ^{6}Li should be simultaneously depleted. In the parameter region, $\tau_X \sim 10^8$–10^{12} s and $\zeta_X \sim 10^{-13}$–10^{-12} GeV, the ^{7}Li abundance is almost unchanged from the SBBN value even should the radiative decay of unstable particles and subsequent nonthermal nucleosynthesis be taken into consideration. Only ^{6}Li is enhanced by about 3 orders of magnitude higher than the SBBN value. This enhancement can be as much as several times the observed ^{6}Li abundance in MPHSs. Hence, the present scenario remains a viable possibility for ^{6}Li enhancement if the true depletion mechanisms or other systematic effects lead to approximately the same degree of depletion for both ^{6}Li and ^{7}Li.

In summary, we have found a parameter region of $\tau_X \sim 10^8$–10^{12} s and $\zeta_X \sim 10^{-13}$–10^{-12} GeV where the nonthermal nucleosynthesis of ^{6}Li can explain the observed abundance level in MPHSs. This parameter region satisfies the two observational constraints on the CMB energy spectrum and the primordial light-element abundances, although it cannot be a solution to the small-scale structure problem.

It is very fascinating to consider the possibility that such new physics as the decay of exotic particles plays a role in producing the observed abundances of lithium in the universe. Clearly, further research into lithium nucleosynthesis and the interpretation of the ^{6}Li plateau would be very valuable. Also, further observations of the ^{6}Li abundances in the stellar atmosphere of MPHSs will help to constrain the various suggested candidates for ^{6}Li production and to answer the question as to whether it is synthesized cosmologically or by cosmic ray interactions in the Galaxy.

[1] D. N. Spergel *et al.* (WMAP Collaboration), Astrophys. J. Suppl. Ser. **148**, 175 (2003).

[2] D. N. Spergel *et al.*, astro-ph/0603449.

[3] J. Ellis, D. V. Nanopoulos, and S. Sarkar, Nucl. Phys. B **259**, 175 (1985).

[4] M. H. Reno and D. Seckel, Phys. Rev. D **37**, 3441 (1988).

[5] S. Dimopoulos, R. Esmailzadeh, G. D. Starkman, and L. J. Hall, Phys. Rev. Lett. **60**, 7 (1988); S. Dimopoulos, R. Esmailzadeh, L. J. Hall, and G. D. Starkman, Astrophys. J. **330**, 545 (1988); Nucl. Phys. B **311**, 699 (1989).

[6] M. Y. Khlopov, Y. L. Levitan, E. V. Sedelnikov, and I. M. Sobol, Phys. At. Nucl. **57**, 1393 (1994); E. V. Sedelnikov, S. S. Filippov, and M. Y. Khlopov, Phys. At. Nucl. **58**, 235 (1995).

[7] K. Jedamzik, Phys. Rev. Lett. **84**, 3248 (2000).

[8] M. Kawasaki, K. Kohri, and T. Moroi, Phys. Rev. D **63**, 103502 (2001).

[9] R. H. Cyburt, J. Ellis, B. D. Fields, and K. A. Olive, Phys. Rev. D **67**, 103521 (2003).

[10] K. Jedamzik, Phys. Rev. D **70**, 063524 (2004).

[11] K. Jedamzik, Phys. Rev. D **70**, 083510 (2004).

[12] M. Kawasaki, K. Kohri, and T. Moroi, Phys. Rev. D **71**, 083502 (2005).

[13] K. Jedamzik, hep-ph/0604251.

[14] J. L. Feng, A. Rajaraman, and F. Takayama, Phys. Rev. Lett. **91**, 011302 (2003).

[15] G. Servant and T. M. P. Tait, Nucl. Phys. B **650**, 391 (2003).

[16] S. G. Ryan, T. C. Beers, K. A. Olive, B. D. Fields, and J. E. Norris, Astrophys. J. **530**, L57 (2000).

[17] J. Melendez and I. Ramirez, Astrophys. J. **615**, L33 (2004).

[18] E. Rollinde, E. Vangioni-Flam, and K. A. Olive, Astrophys. J. **627**, 666 (2005).

[19] K. Jedamzik, K. Y. Choi, L. Roszkowski, and R. Ruiz de Austri, hep-ph/0512044.

[20] J. R. Ellis, K. A. Olive, and E. Vangioni, Phys. Lett. B **619**, 30 (2005).

[21] M. Kawasaki and T. Moroi, Astrophys. J. **452**, 506 (1995).

[22] R. J. Protheroe, T. Stanev, and V. S. Berezinsky, Phys. Rev. D **51**, 4134 (1995).

[23] V. S. Berezinskii, S. V. Bulanov, V. A. Dogiel, V. L. Ginzburg, and V. S. Ptuskin, in *Astrophysics of Cosmic Rays*, edited by V. S. Verezinskii and V. L. Ginzburg (North-Holland, New York, 1990).

[24] J. P. Meyer, Astron. Astrophys. Suppl. Ser. **7**, 417 (1972).

[25] H. Reeves, Annu. Rev. Astron. Astrophys. **12**, 437 (1974).

[26] M. A. Famiano, R. N. Boyd, and T. Kajino, Astrophys. J. **576**, 89 (2002).

[27] S. N. Abramovich, B. Ja. Guzhovskij, V. A. Zherebcov, and A. G. Zvenigorodskij, Annual Vop. At. Nauki i Tekhn., Ser. Yadernye Konstanty **4**, 17 (1984).

[28] M. Asplund, D. L. Lambert, P. E. Nissen, F. Primas, and V. V. Smith, astro-ph/0510636.

[29] D. Kirkman, D. Tytler, N. Suzuki, J. M. O'Meara, and D. Lubin, Astrophys. J. Suppl. Ser. **149**, 1 (2003).

[30] H. W. Moos *et al.*, Astrophys. J. Suppl. Ser. **140**, 3 (2002).

[31] T. M. Bania, R. T. Rood, and D. S. Balser, Nature (London) **415**, 54 (2002).

[32] J. Geiss and G. Gloeckler, Space Sci. Rev. **84**, 239 (1998).

[33] G. Gloeckler and J. Geiss, Space Sci. Rev. **84**, 275 (1998).

[34] H. Busemann, F. Bühler, A. Grimberg, V. S. Heber, Y. N. Agafonov, H. Baur, P. Bochsler, N. A. Eismont, R. Wieler, and G. N. Zastenker, Astrophys. J. **639**, 246 (2006).

[35] C. Chiappini, A. Renda, and F. Matteucci, Astron. Astrophys. **395**, 789 (2002).

[36] E. Vangioni-Flam, K. A. Olive, B. D. Fields, and M. Casse, Astrophys. J. **585**, 611 (2003).

[37] Y. I. Izotov and T. X. Thuan, Astrophys. J. **602**, 200 (2004).

[38] K. A. Olive and E. D. Skillman, Astrophys. J. **617**, 29 (2004).

[39] D. L. Lambert, AIP Conf. Proc. **743**, 206 (2004).

[40] C. Charbonnel and F. Primas, Astron. Astrophys. **442**, 961 (2005).

[41] D. Yong, B. W. Carney, W. Aoki, A. McWilliam, and W. J. Schuster, in *Proceedings of the International Symposium on Origin of Matter and Evolution of Galaxies held at Tokyo, Japan, 2005* (American Institute of Physics, New York, to be published).

[42] O. Richard, G. Michaud, and J. Richer, Astrophys. J. **619**, 538 (2005).

[43] T. K. Suzuki and S. Inoue, Astrophys. J. **573**, 168 (2002).

[44] S. Inoue, W. Aoki, T. K. Suzuki, S. Kawanomoto, A. E. García-Pérez, S. G. Ryan, and M. Chiba, IAU Symposium / Symp-Int Astron Union **228**, 59 (2005).

[45] E. Rollinde, E. Vangioni, and K. A. Olive, astro-ph/0605633.

[46] N. Prantzos, astro-ph/0510122.

[47] M. Pospelov, hep-ph/0605215.

[48] A. Coc, E. Vangioni-Flam, P. Descouvemont, A. Adahchour, and C. Angulo, Astrophys. J. **600**, 544 (2004).

[49] L. H. Kawano, FERMILAB Report No. FERMILAB-Pub-92/04-A (1992).

[50] G. J. Mathews, T. Kajino, and T. Shima, Phys. Rev. D **71**, 021302(R) (2005).

[51] W. Hu and J. Silk, Phys. Rev. Lett. **70**, 2661 (1993).

[52] W. Hu and J. Silk, Phys. Rev. D **48**, 485 (1993).

[53] K. Hagiwara, *et al.* (Particle Data Group), Phys. Rev. D **66**, 010001 (2002).

[54] J. L. Feng, A. Rajaraman, and F. Takayama, Phys. Rev. D **68**, 063504 (2003).

[55] M. Viel, J. Lesgourgues, M. G. Haehnelt, S. Matarrese, and A. Riotto, Phys. Rev. D **71**, 063534 (2005).

[56] R. Barkana, Z. Haiman, and J. P. Ostriker, Astrophys. J. **558**, 482 (2001).

[57] N. Yoshida, A. Sokasian, L. Hernquist, and V. Springel, Astrophys. J. **591**, L1 (2003).

[58] J. A. R. Cembranos, J. L. Feng, A. Rajaraman, and F. Takayama, Phys. Rev. Lett. **95**, 181301 (2005).

[59] http://arcade.gsfc.nasa.gov.

[60] A. Kogut *et al.*, Astrophys. J. Suppl. Ser. **154**, 493 (2004).